Materials and Design 181 (2019) 107982

Contents lists available at ScienceDirect

Materials and Design

journal homepage: www.elsevier.com/locate/matdes

Flexible and tunable electromagnetic meta-atom based on silver nanowire networks

Chang Liu [a], Jun Cai [a,*], Xinghao Li [a], Wenqiang Zhang [b], Deyuan Zhang [a]

[a] School of Mechanical Engineering and Automation, Beihang University, Beijing 100191, China
[b] College of Engineering, China Agricultural University, Beijing 100191, China

HIGHLIGHTS

- The meta-atom is composed of split ring resonator-based silver nanowire networks onto a biaxially pre-stretched PDMS film.
- Split ring resonator of biaxially pre-stretched sample has excellent deformation potential due to its ridge-like structures.
- The flexible metal split ring resonator maintains good electrical properties even when the meta-atom is stretched to 100%.
- Mechanically tunable performance of the prepared meta-atom with silver nanowire (600 mg/m^2) covers as much as 90% of X-band.

GRAPHICAL ABSTRACT

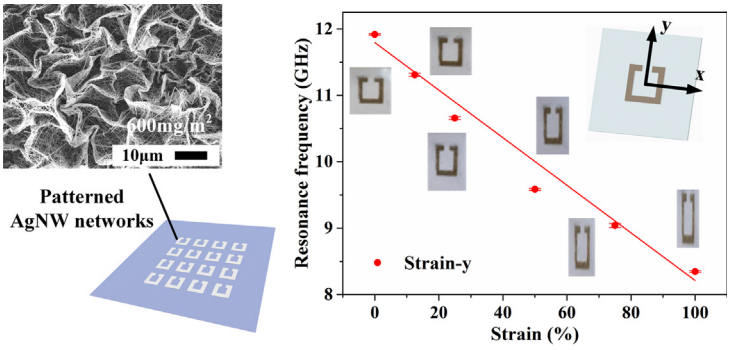

ARTICLE INFO

Article history:
Received 9 April 2019
Received in revised form 25 June 2019
Accepted 27 June 2019
Available online 28 June 2019

Keywords:
Electromagnetic interference shielding
Flexible
Stretchable
Tunable electromagnetic meta-atom
Split ring resonator
Silver nanowire networks

ABSTRACT

Electromagnetic interference (EMI) shielding metamaterials have become indispensable in reducing electromagnetic (EM) wave radiation pollution. In this study, a flexible and tunable EM meta-atom was proposed and fabricated for EMI shielding metamaterials. The meta-atom was composed of a split ring resonator made with silver nanowire (AgNW) networks attached onto a biaxially pre-stretched poly(dimethylsiloxane) film. The structures and morphologies of samples prepared under different pre-stretching conditions showed that the AgNW networks on the biaxially pre-stretched samples are more stable than those on the unstretched and uniaxially pre-stretched samples. This endowed the meta-atoms with excellent electrical conductivity and reliability under various strain conditions. The tunable performance of the as-prepared materials with an AgNW area density of 600 mg/m^2 was remarkable, covering as much as 90% of the entire X-band (8–12 GHz). This strategy could open new avenues toward the development of reconfigurable EMI shielding metamaterials, particularly for the wide-frequency range applications.
© 2019 The Authors. Published by Elsevier Ltd. This is an open access article under the CC BY-NC-ND license (http://creativecommons.org/licenses/by-nc-nd/4.0/).

1. Introduction

In recent years, the severe electromagnetic (EM) wave radiations are threatening human health and affecting the operational stability of sensitive electric devices [1–5]. To address these limitations, researchers have explored different strategies, and the development of highly

* Corresponding author.
E-mail address: jun_cai@buaa.edu.cn (J. Cai).

https://doi.org/10.1016/j.matdes.2019.107982
0264-1275/© 2019 The Authors. Published by Elsevier Ltd. This is an open access article under the CC BY-NC-ND license (http://creativecommons.org/licenses/by-nc-nd/4.0/).

efficient and strongly adaptable electromagnetic interference (EMI) shielding materials is the main approach [6,7]. Diverse EMI shielding materials have been developed in the past decades [8,9], and some of them have been successfully applied in civil and military fields. Among these, metamaterials have attracted significant attention because of their useful special properties such as negative permeability [10,11] and left-handed electromagnetism [12,13]. This has led to intense theoretical, computational, and experimental investigation of the unique phenomena, such as superlensing [14], cloaking [15], and other metamaterial-based resonant devices [16–18]. In particular, split ring resonator (SRR) has been extensively used as a magnetic resonance structure [18–21]. EMI shielding metamaterials made with SRRs exhibit a fast response and good feasibility. Some tunable metamaterial strategies have been proposed [16,22]. Typically, tunable technologies can be classified into three categories based on the tuning mechanism. First method involves changing the effective parameter (conductance or inductance) of the unit cell by embedding additional electronic components [23–25]. These metamaterials have a stable tuning ability; however, their environmental adaptability is poor because of their complex structure. Second technology involves the replacement of materials or alteration of the constituent material properties of the unit cell [26–28]. In this case, a stable and ideal adjustment of the properties is yet to be achieved. Third method constitutes altering the structural parameters of the unit cell [29–31]. This mechanically tunable technology is convenient and highly efficient. However, it is difficult to realize a wide tunable range for EMI shielding metamaterials because of the contradiction between electrical stability and structural deformation.

If unit cells can be fabricated with stretchable conductive materials, we can alter the structures of the unit cells at a larger scale for deformation and simultaneously retain their electrical conductivity, to achieve frequency-tunable metamaterials with a wide tunable performance. Different stretchable electrodes have been developed by adding various conductive fillers into the matrix in the flexible electronics field such as conducting polymers [32], carbon nanotubes [33,34], graphene [35], and metallic nanowires [36–41]. Among these, silver nanowires (AgNWs) with a high aspect ratio are promising candidates for flexible and stretchable electronics [38–41]. Therefore, these have been considered for preparing stretchable unit cells.

In this research, a flexible and tunable EM meta-atom was designed by performing extensive simulations using the CST STUDIO SUITE software. The high aspect-ratio AgNWs dispersed in ethanol were collected by a vacuum filtration method, during which a constraint mold was used to obtain the designed metal SRR composed of AgNWs. Thereafter, these were transferred onto a biaxially pre-stretched poly(dimethylsiloxane) (PDMS) film to fabricate the desired tunable EM meta-atom. To our knowledge, this is the first report of the fabrication of SRRs using the patterned filtration method, which is simple and effective, and the pre-stretched PDMS base endows them with high deformability. The morphologies of the AgNW networks under different pre-stretched conditions were investigated. Furthermore, the electrical properties and tunable EM properties of as-prepared samples under various strain conditions were studied.

2. Experimental

2.1. Materials

The AgNW ethanol solution of 5 mg/ml was purchased from JCNANO Tech Co., Ltd., China. The average diameter and length of the nanowires were 90 nm and 200 μm, respectively. PDMS (Sylgard 184) was supplied by Dow Corning. Nylon filters were purchased from JinTeng Laboratory Equipment Co., Ltd., China. Ethanol was used to further disperse AgNW solution, and was purchased from Beijing Chemical Works.

2.2. Design and fabrication

The CST STUDIO SUITE software (Dassault Systemes) was employed to investigate the design of meta-atom. In the simulation configuration process, a brick component was built with X_{max}-X_{min} of 22.86 mm, Y_{max}-Y_{min} of 10.16 mm, and Z_{max}-Z_{min} of 100 mm, which was set as the vacuum material, and an incident EM wave travelled along the z direction. The boundary conditions of a perfect electric conductor were utilized along both x and y directions. To determine the transmission coefficient in simulation, a frequency domain solver was used. The simulations were conducted in the frequency range of 1–18 GHz. A flexible and tunable meta-atom was finally designed to operate in the X-band (8–12 GHz) by conducting extensive simulations. The designed metal SRR had a square structure with an outer side length (l_1) of 3.8 mm, inner side length (l_2) of 2.8 mm, gap distance (d) of 1.2 mm, and thickness of approximately 1 μm (Fig. 2), which was on the wave-transparent polymer substrate.

A schematic of the fabrication process of mechanically tunable meta-atoms is shown in Fig. 1. Initially, a PDMS film (approximately 200 μm in thickness), obtained by a spin coating process (1200 rpm; 30 s), was fixed pointwise on a custom-made biaxial stretching apparatus and stretched to double its original length uniformly in the orthogonal direction. In a parallel process, the vacuum filtration method was employed to collect the AgNWs on a nylon filter, and the AgNW networks could be patterned into various shapes with a shadow mask. Thus, the patterned AgNW networks with area densities of 12.5, 25, 50, 100, and 150 mg/m^2 were obtained using the designed SRR shadow mask. The nylon filter was then placed on the biaxially pre-stretched PDMS film by applying a uniform pressure of approximately 150 kPa for 2 min. The patterned AgNW networks were transferred completely after carefully lifting the nylon filter. Finally, the mechanically tunable meta-atoms were fabricated after releasing the biaxial stretching force. The area densities of the samples were 50, 100, 200, 400, and 600 mg/m^2 as the PDMS shrank. For comparison with other pre-stretched conditions, both the uniaxially pre-stretched (100%) and unstretched samples with an area density of 600 mg/m^2 were also fabricated.

2.3. Characterization and measurement

The morphologies and structures of biaxially pre-stretched, uniaxially pre-stretched and unstretched samples were investigated using a scanning electron microscope (SEM, JEOL JSM 6010). The resistances of the flexible metal SRRs with different area densities were analyzed under varying strain conditions by a source meter (Keithley 2410). The transmittances of the mechanically tunable meta-atoms with various strain conditions were measured for the X-band using a vector network analyzer (AV3672B) and a rectangular waveguide (WR90, 22.86 × 10.16 mm).

3. Results and discussion

3.1. Simulation of the meta-atom

To assess the tuning ability of the mechanically tunable meta-atom, the designed meta-atom was investigated by many simulations that replicated the proposed experimental setup. As shown in Fig. 2a, the SRR is made of a flexible silver material and adhered to a highly stretchable PDMS substrate. The meta-atom is fixed along the x-y plane inside the waveguide, and the EM waves propagate in the z direction; the waves penetrate the flexible metal SRR. This configuration of the SRR inside the test waveguide has been proven to induce magnetic resonance [42]. With the designed geometrical parameters, the simulated resonance frequency of the meta-atom is 11.848 GHz. Fig. 2b shows the

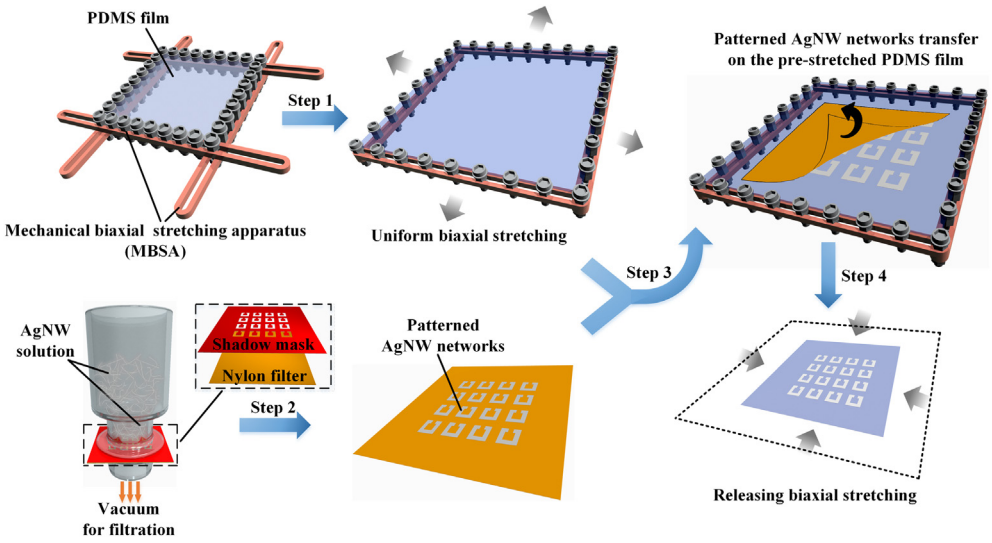

Fig. 1. Schematic of the fabrication process of mechanically tunable meta-atoms.

magnitude of the electric field distribution at the resonance frequency. When the meta-atom is stretched to 150% of the original length along the x direction, the resonance frequency decreases from 11.848 GHz (Fig. 2c) to 9.646 GHz (Fig. 2d). The resonant responses of the SRRs can be simply expressed with an equivalent LC oscillator circuit. The resonant frequency is determined by the inductance L and capacitance C resulting from the current path and the split gap of the SRR, respectively, as shown in Eq. (1) [43,44].

$$f_r = \frac{1}{2\pi\sqrt{LC}} \tag{1}$$

Therefore, varying the structure of the SRR by applying a uniaxial mechanical stretch will cause changes in the equivalent electrical properties because of changes in L and C. The mechanically tunable mechanism is only conceptually illustrated. We demonstrate and analyze more quantitative simulation results combined with experimental results in the following section.

3.2. Morphologies and structures of the SRRs

The morphologies and structures of the biaxially pre-stretched, uniaxially pre-stretched, and unstretched samples are shown in Fig. 3. Fig. 3a and b shows the SEM images of the unstretched samples (600 mg/m^2) under no strain and 10% strain of the PDMS film, respectively. As the AgNW network and PDMS film are stretched, cracks are observed in the flexible metal SRRs even at a stretching ratio of only 10%. The number of cracks and the gaps between them gradually increase with increase in the stretching percentage, indicating poor stretchability of the unstretched samples. This shows that these samples

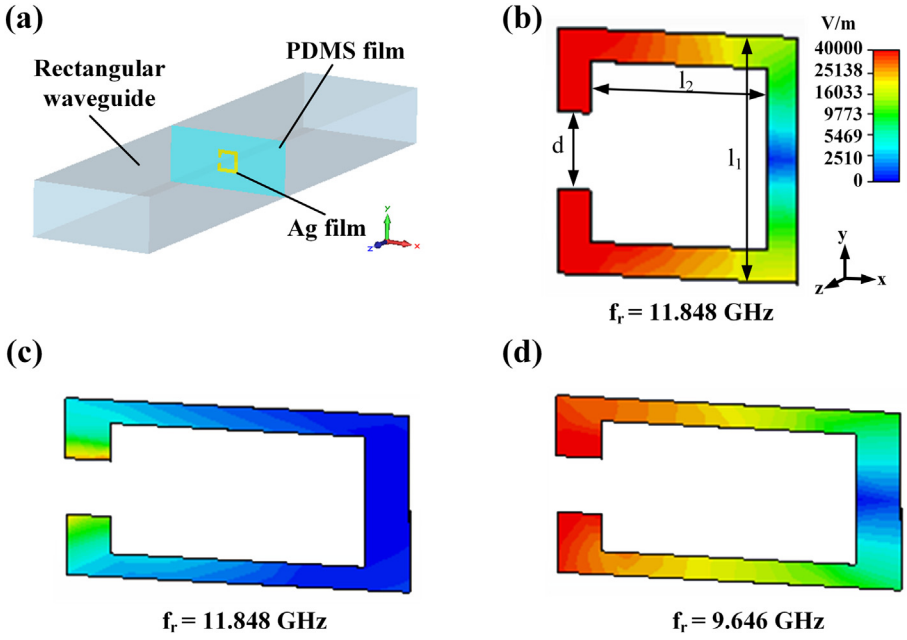

Fig. 2. Simulation of electric field magnitude distribution for flexible metal SRR: (a) Model created in CST studio suite software; electric field magnitude of the designed SRR at a frequency of (b) 11.848 GHz under no strain, (c) 11.848 GHz under 50% strain, (d) 9.646 GHz under 50% strain.

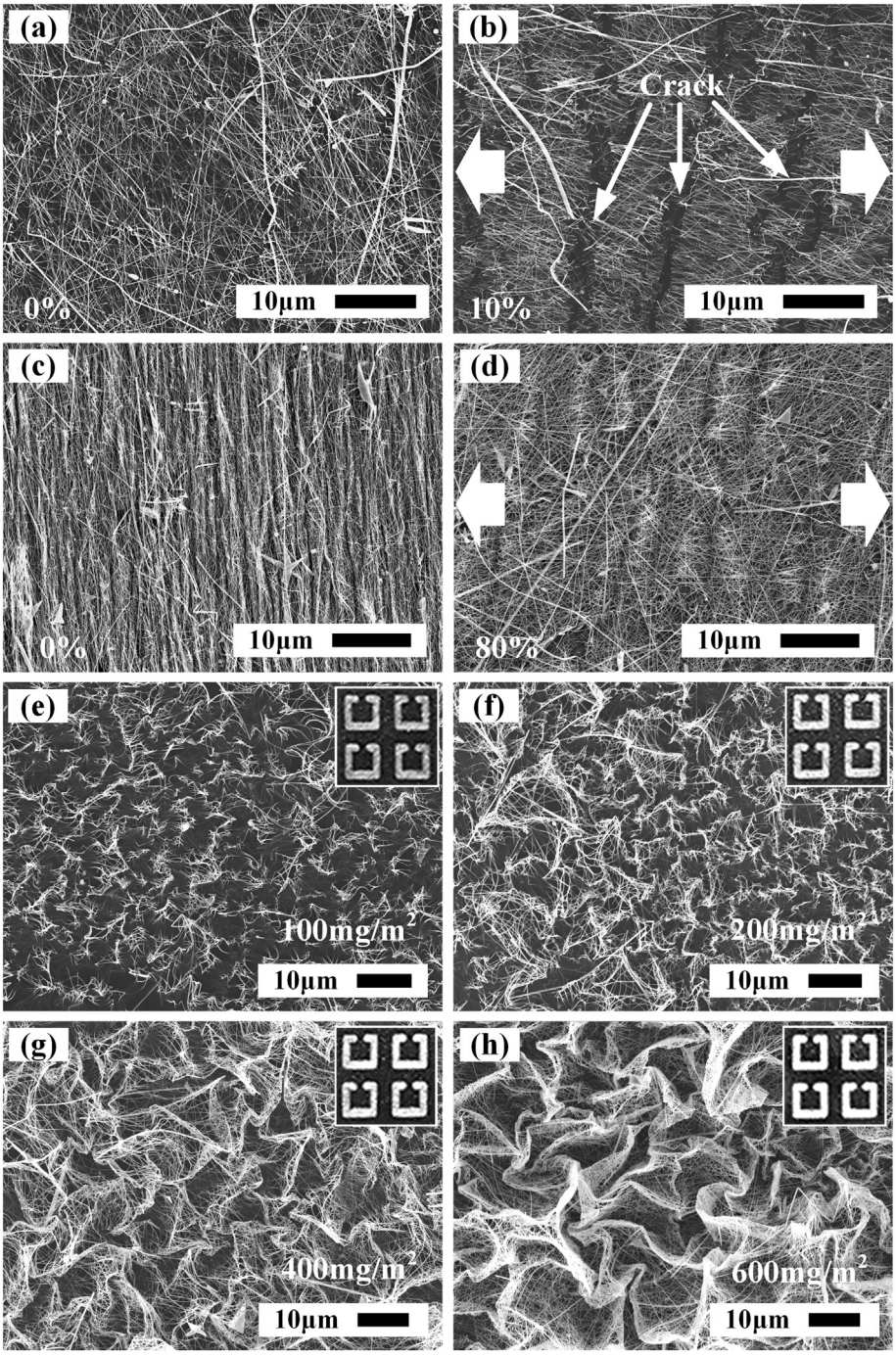

Fig. 3. SEM images of the flexible metal SRRs based on AgNW networks under different conditions. (a and b) Unstretched samples with area density of 600 mg/m^2 for stretch ratios of 0 and 10%. (c and d) Uniaxially pre-stretched samples with area density of 600 mg/m^2 for stretch ratios of 0 and 80% along the pre-stretched direction. (e–h) Biaxially pre-stretched samples with area densities of 100, 200, 400, and 600 mg/m^2.

are unsuitable for mechanical tuning. Fig. 3c and d shows the morphologies of the AgNW networks on the uniaxially pre-stretched PDMS film under different strain conditions. Fig. 3c shows nearly periodical wrinkle structures formed by uniaxially stretching and shrinking the PDMS film. The wrinkle structures unfolded when the uniaxially pre-stretched PDMS film was stretched along the pre-stretched direction. Even when the PDMS film is stretched by 80%, the flexible metal SRRs remain intact and continuous, as shown in Fig. 3d. This shows that the pre-stretched substrate can serve as a basis for applying AgNWs to mechanically tunable fields, as is consistent with previous reports [41]. However, the uniaxially pre-stretched samples exhibited poor stretching capacity except in the pre-stretched direction, and when a deformation occurred in any other direction, cracks similar to those shown in Fig. 3b were generated. Thus, to attain excellent stretching capacity of the flexible metal SRRs in all directions, we attempted to stretch and shrink the PDMS film along two orthogonal directions simultaneously (Fig. 2). Fig. 3e–h shows the morphologies of the biaxially pre-stretched samples, and their AgNW area densities are 100, 200, 400, and 600 mg/m^2. Unlike the periodicity of the wrinkles on the uniaxially pre-stretched samples, the biaxially pre-stretched samples

have wavy mountain-like structures with crumpled wrinkles appearing as ridges. The AgNW networks are denser, and the wrinkles are more distinct with increase in area density, indicating greater deformation potential.

3.3. Electrical properties of the SRRs

Generally, the electrical properties of flexible metal SRRs under various strain conditions play a dominant role in their mechanical tunability. Therefore, the electromechanical stabilities of the flexible metal SRRs were analyzed by conducting repeated strain tests. A cyclic strain test apparatus was established, and liquid metal was applied during the entire course of the cyclic strain test to ensure good conductive connection, as shown in Fig. S2 (Supporting Information). The strain is defined as $\varepsilon = (L - L_0)/L_0$, where L_0 is the initial length of the measured meta-atom samples between two clamped positions, and L is the changed length under various strain conditions. The length change can be precisely controlled using the controller of the cyclic strain test apparatus. Further, the SRR strain value is approximately equal to that of the meta-atom sample because the SRR layer is extremely thin in contrast with the PDMS substrate, which is in accordance with extant reports for the calculation method [38,41]. Fig. 4a shows the curves for the resistance change measured up to 100% strain for the first five cycles in either direction. The resistance values were measured in steps of 5% strain. The initial resistance values of the flexible metal SRRs based on the AgNW networks are 52.153, 38.120, 23.224, 6.160, and 3.473 Ω for area densities of 50, 100, 200, 400, and 600 mg/m^2, respectively. The flexible metal SRRs based on the AgNW networks retain their electrical conductivity, with only slight changes in the resistances even at high stretch ratios. For example, the original resistance value of the sample of density 400 mg/m^2 (pink curve) was 6.160 Ω for the first cycle; for stretch ratios of 50 and 100%, the resistance values were 9.281 and 13.642 Ω, respectively; the value was 9.720 Ω at the end of the first cycle. Because of the wavy mountain-like structures on the biaxially pre-stretched samples, a vast majority of the AgNW networks maintained their connections during the stretching process. Some of the AgNWs rearranged the network connection. After one stretching cycle, the resistance was higher than the corresponding resistances during the previous cycles at the same stretch ratio under all AgNW area density conditions. This phenomenon resulted from the partially invalid connection of the AgNWs with the flexible metal SRRs during every stretching cycle. In contrast, the resistance under the same strained condition was constant as the number of cycles increased, which is consistent with previous reports [38]. In addition, the resistance gradually stabilized with the increase in the area density of the flexible metal SRRs form 50 to 600 mg/m^2. This is because the area density plays an important role in the formation of conductive paths. When the area density is less than 200 mg/m^2, the alternative conductive path is limited and a larger number of isolated AgNW networks are easily generated as the stretch ratio increases. The resistances of the samples with densities 400 and 600 mg/m^2 were low and nearly constant under various strain conditions. This indicates that multilayer conducting paths are formed for large concentrations of the AgNW. The partially invalid connection of the AgNW networks has a negligible effect on the electrical properties of the samples. As shown in Fig. 4b, the flexible metal SRRs exhibit good stability in terms of the electrical properties, as demonstrated from the cyclic stretching test (1000 cycles). For each test, the SRRs were stretched to 100% strain and released to the initial position at a constant speed, and the resistance values were measured at the end of every 100 cycles. The rate of change in the resistance of the flexible metal SRR increased at the beginning of the cyclic stretching test, and gradually became very stable as the number of stretching cycles increased. That is, the resistance of the flexible metal SRR eventually converged to a constant value after hundreds of cyclic stretching. Moreover, the relationship between the resistance change and the area density of the AgNW was negative when the resistance became stable. For area densities of 50, 100, 200, 400, and 600 mg/m^2, the average value of the stabilized resistance change are 3.010, 2.820, 2.674, 2.532, and 2.502, respectively.

3.4. EM characteristics of meta-atom

The tunable EM characteristics of the meta-atom under various strain conditions and along different directions were investigated using a custom-made biaxial stretching apparatus (Fig. 5a). The meta-atom was made up of an individual SRR taken from the fabricated sample with an AgNW area density of 600 mg/m^2 and was placed between the X-band waveguides. These tested samples had stabilized resistance values after hundreds of cyclic stretching so that the tunable EM characteristics were accurate and stable under various strain conditions. On the one hand, the meta-atom was stretched along the x direction with different stretch ratios. The flexible metal SRR flattened, and the split gap widened. Although the PDMS film exhibited a negative Poisson's ratio, the SRR was still a standard rectangular structure because of the fixation on all sides. The measured results are indicated using solid lines in Fig. 5b; the resonance of the transmittance spectra gradually moves toward the low-frequency direction. The resonance frequency shifted from 11.927 to 11.560, 11.224, 11.014, and 10.804 GHz for stretch ratios of 0, 25, 50, 75, and 100%, respectively. The resonance strength increased with an increase in the stretch ratio. The dotted lines in Fig. 5b indicate the simulated transmittance spectra of the meta-atom. The deformed SRR was modeled using the initial structural parameter and stretch ratio, and the electrical conductivity of the deformed SRR was considered to be unchanged because of the steady

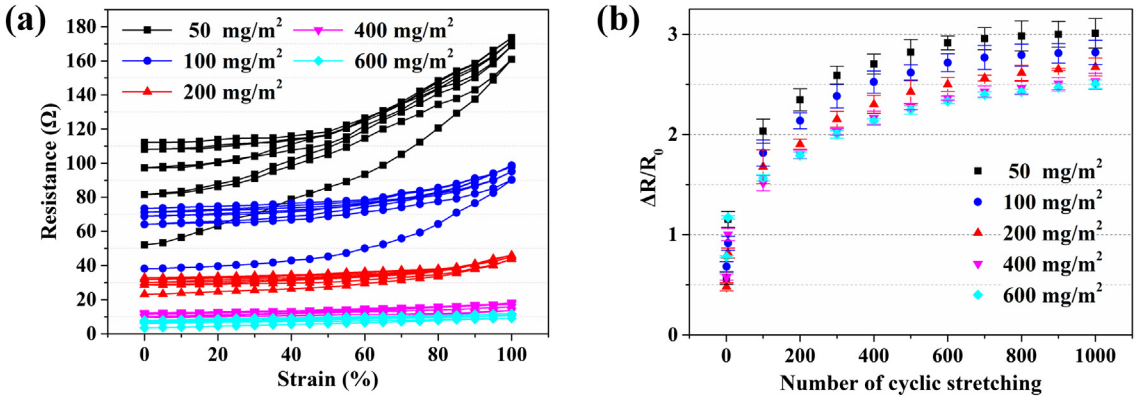

Fig. 4. Electromechanical properties of flexible metal SRRs: (a) Strain-dependent resistance measurement of samples with different area densities during five stretching cycles. (b) Resistance changes of samples with different area densities with respect to cyclic stretching.

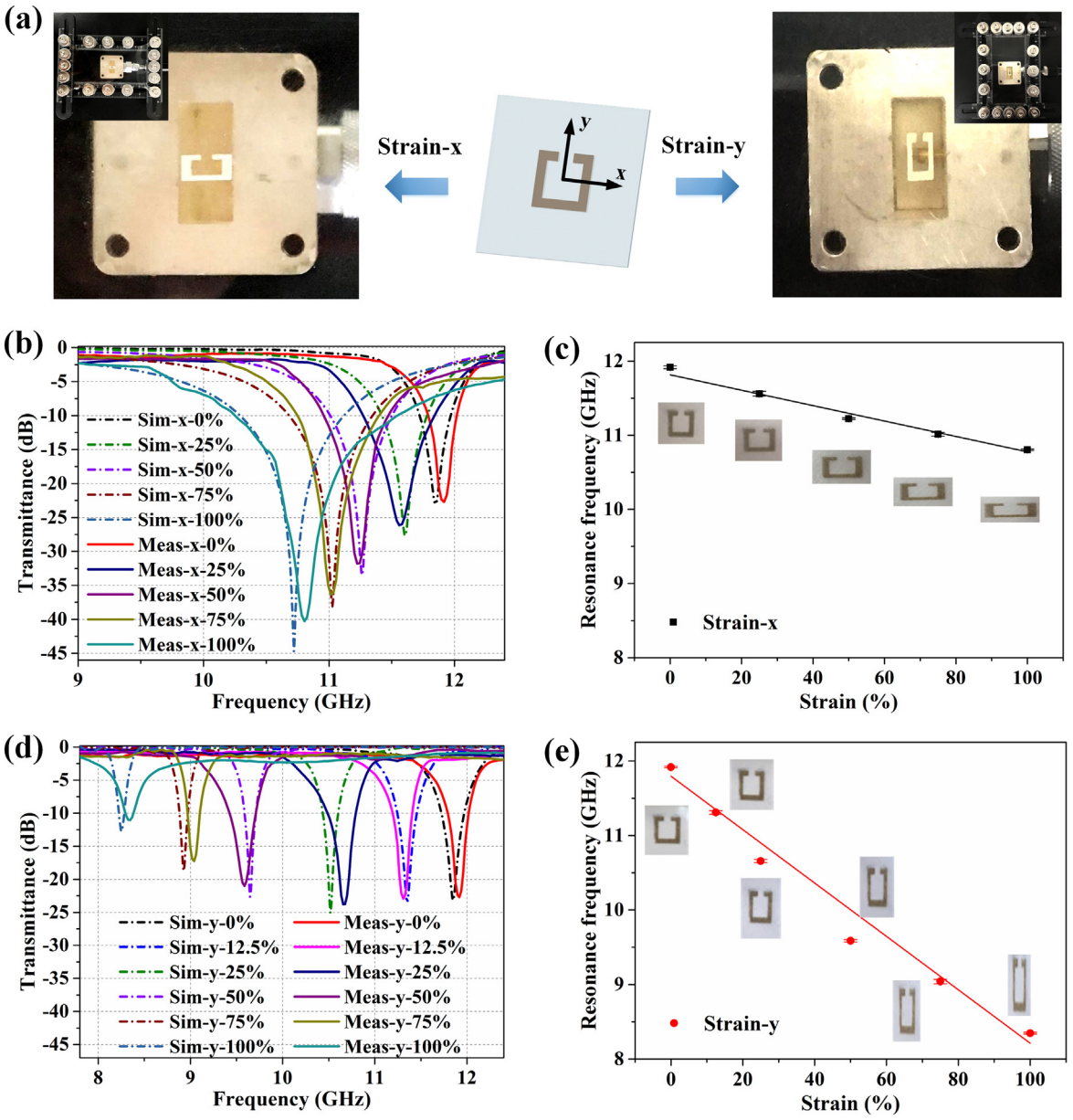

Fig. 5. Tunable EM characteristics under various strain conditions: (a) Digital images of tunable EM characteristic test under x-strain and y-strain. (b) and (d) Measured and simulated transmittance spectra of the tunable meta-atom in the strain range of 0–50% strain along the x and y directions, respectively. (c) and (e) Resonance frequency as a function of the stretch ratio for the tunable meta-atom along the x and y directions, respectively.

electrical property of the used sample (600 mg/m^2). The transmittance of the SRR under various strain conditions was largely in good agreement with the simulated results. On the other hand, the meta-atom was stretched under various strain conditions along the y direction. The flexible metal SRR exhibited a lanky structure and a narrower split gap. Fig. 5d shows the measured (solid line) and simulated (dotted line) results of the deformed SRR. At stretch levels of 0, 12.5, 25, 50, 75, and 100%, the resonance frequencies through the actual measurement were 11.927, 11.308, 10.657, 9.586, 9.040 and 8.337 GHz, respectively. A simple uniaxial stretching (up to 100%) of the flexible metal SRR could achieve a continuous tuning process for over 90% of the X-band. The experimental EM measurement results showed good agreement with the simulated results. The minimal discrepancy between the simulated and measured results demonstrates the precision in fabricating the flexible metal SRRs; moreover, this shows that the stretching measurement is acceptable. Fig. 5c and e summarizes the relationships between the strains and the measured resonance frequency through three sets of measured results. The relationship is largely linear when the meta-atom is stretched along either the x direction or y direction, and different samples exhibit good reproducibility. Furthermore, the same SRR exhibits different resonance frequencies under different stretch ratios, along different directions. Thus, the meta-atoms based on the AgNW networks exhibit excellent mechanically tunable properties.

4. Conclusion

In conclusion, we designed a flexible and tunable EM meta-atom to operate in the X-band (8–12 GHz) using the CST STUDIO SUITE software. To the best of our knowledge, the meta-atom was developed by preparing a flexible metal SRR based on the AgNW networks onto a biaxially pre-stretched PDMS film via the vacuum filtration method for the first time. The flexible metal SRRs with a low area density have excellent conductivity and electromechanical stability. We also

demonstrated that a simple uniaxial stretching of the meta-atom with an AgNW area density of 600 mg/m^2 could achieve a continuous tuning process for over 90% of the X-band. The measured results are similar to the simulated results, which validates the reliability of our design and theoretical analysis. The proposed meta-atom presents a simple and effective element for realizing mechanically tunable EM metamaterials, which might open new directions toward reconfigurable EMI shielding metamaterials. Moreover, these promising metamaterials exhibit good environmental adaptability and property stability and can benefit EM applications, such as wearable EM devices, flexible EM protection skin, and EM frequency-tunable materials.

Credit author statement

Chang Liu designed the tunable mate-atom and performed the simulations. Chang Liu and Xinghao Li fabricated the samples and analyzed their morphologies, electrical properties, and tunable performance. Chang Liu, Jun Cai, Xinghao Li, and Wenqiang Zhang prepared the manuscript. Jun Cai and Deyuan Zhang supervised the project.

Notes

The authors declare no competing financial interest.

Acknowledgments

This work was supported by the National Natural Science Foundation of China (Grant No. 51775022) and the Fundamental Research Funds for the Central Universities.

Appendix A. Supplementary data

Supplementary data to this article can be found online at https://doi.org/10.1016/j.matdes.2019.107982.

References

[1] F. Shahzad, M. Alhabeb, C.B. Hatter, B. Anasori, S. Man Hong, C.M. Koo, Y. Gogotsi, Electromagnetic interference shielding with 2D transition metal carbides (MXenes), Science 353 (6304) (2016) 1137–1140, https://doi.org/10.1126/science.aag2421.
[2] S. Kashi, R.K. Gupta, T. Baum, N. Kao, S.N. Bhattacharya, Dielectric properties and electromagnetic interference shielding effectiveness of graphene-based biodegradable nanocomposites, Mater. Des. 109 (2016) 68–78, https://doi.org/10.1016/j.matdes.2016.07.062.
[3] Y. Zhang, Y. Huang, T. Zhang, H. Chang, P. Xiao, H. Chen, Z. Huang, Y. Chen, Broadband and tunable high-performance microwave absorption of an ultralight and highly compressible graphene foam, Adv. Mater. 27 (12) (2015) 2049–2053, https://doi.org/10.1002/adma.201405788.
[4] C. Liu, J. Cai, Y. Duan, X. Li, D. Zhang, Aligning flaky FeSiAl particles with a two-dimensional rotating magnetic field to improve microwave-absorbing and shielding properties of composites, J. Magn. Magn. Mater. 458 (2018) 116–122, https://doi.org/10.1016/j.jmmm.2018.02.091.
[5] H. Mei, X. Zhao, J. Xia, F. Wei, D. Han, S. Xiao, L. Cheng, Compacting CNT sponge to achieve larger electromagnetic interference shielding performance, Mater. Des. 144 (2018) 323–330, https://doi.org/10.1016/j.matdes.2018.02.047.
[6] S. Geetha, K.K. Satheesh Kumar, C.R.K. Rao, M. Vijayan, D.C. Trivedi, EMI shielding: methods and materials-a review, J. Appl. Polym. Sci. 112 (4) (2009) 2073–2086, https://doi.org/10.1002/app.29812.
[7] L.B. Kong, Z.W. Li, L. Liu, R. Huang, M. Abshinova, Z.H. Yang, C.B. Tang, P.K. Tan, C.R. Deng, S. Matitsine, Recent progress in some composite materials and structures for specific electromagnetic applications, Int. Mater. Rev. 58 (4) (2013) 203–259, https://doi.org/10.1179/1743280412y.0000000011.
[8] A. Kausar, I. Rafique, B. Muhammad, Electromagnetic interference shielding of polymer/nanodiamond, polymer/carbon nanotube, and polymer/nanodiamond–carbon nanotube nanobifiller composite: a review, Polym. Plast. Technol. Eng. 56 (4) (2016) 347–363, https://doi.org/10.1080/03602559.2016.1233273.
[9] S. Maity, A. Chatterjee, Conductive polymer-based electro-conductive textile composites for electromagnetic interference shielding: a review, J. Ind. Text. 47 (8) (2016) 2228–2252, https://doi.org/10.1177/1528083716670310.
[10] H.T. Chen, W.J. Padilla, J.M. Zide, A.C. Gossard, A.J. Taylor, R.D. Averitt, Active terahertz metamaterial devices, Nature 444 (7119) (2006) 597–600, https://doi.org/10.1038/nature05343.
[11] K. Sun, R.H. Fan, Z.D. Zhang, K.L. Yan, X.H. Zhang, P.T. Xie, M.X. Yu, S.B. Pan, The tunable negative permittivity and negative permeability of percolative Fe/Al_2O_3 composites in radio frequency range, Appl. Phys. Lett. 106 (17) (2015), 172902. https://doi.org/10.1063/1.4918998.
[12] N.I. Zheludev, Y.S. Kivshar, From metamaterials to metadevices, Nat. Mater. 11 (11) (2012) 917–924, https://doi.org/10.1038/nmat3431.
[13] S. Zhang, J. Zhou, Y.S. Park, J. Rho, R. Singh, S. Nam, A.K. Azad, H.T. Chen, X. Yin, A.J. Taylor, X. Zhang, Photoinduced handedness switching in terahertz chiral metamolecules, Nat. Commun. 3 (2012), 942. https://doi.org/10.1038/ncomms1908.
[14] N. Kaina, F. Lemoult, M. Fink, G. Lerosey, Negative refractive index and acoustic superlens from multiple scattering in single negative metamaterials, Nature 525 (7567) (2015) 77–81, https://doi.org/10.1038/nature14678.
[15] D. Schurig, J.J. Mock, B.J. Justice, S.A. Cummer, J.B. Pendry, A.F. Starr, D.R. Smith, Metamaterial electromagnetic cloak at microwave frequencies, Science 314 (5801) (2006) 977, https://doi.org/10.1126/science.1133628.
[16] K. Fan, W.J. Padilla, Dynamic electromagnetic metamaterials, Mater. Today 18 (1) (2015) 39–50, https://doi.org/10.1016/j.mattod.2014.07.010.
[17] H. Jeong, T.T. Nguyen, S. Lim, Subwavelength metamaterial unit cell for low-frequency electromagnetic absorber applications, Sci. Rep. 8 (1) (2018), 16774. https://doi.org/10.1038/s41598-018-35267-w.
[18] Q. Li, Z. Tian, X. Zhang, N. Xu, R. Singh, J. Gu, P. Lv, L.-B. Luo, S. Zhang, J. Han, W. Zhang, Dual control of active graphene–silicon hybrid metamaterial devices, Carbon 90 (2015) 146–153, https://doi.org/10.1016/j.carbon.2015.04.015.
[19] L. Jing, Z. Wang, B. Zheng, H. Wang, Y. Yang, L. Shen, W. Yin, E. Li, H. Chen, Kirigami metamaterials for reconfigurable toroidal circular dichroism, NPG Asia Mater 10 (9) (2018) 888–898, https://doi.org/10.1038/s41427-018-0082-x.
[20] G. Yang, X. Liu, Y. Lv, J. Fu, Q. Wu, X. Gu, Broadband polarization-insensitive absorber based on gradient structure metamaterial, J. Appl. Phys. 115 (17) (2014), 17E523. https://doi.org/10.1063/1.4868090.
[21] K. Qiu, J. Jin, Z. Liu, F. Zhang, W. Zhang, A novel thermo-tunable band-stop filter employing a conductive rubber split-ring resonator, Mater. Des. 116 (2017) 309–315, https://doi.org/10.1016/j.matdes.2016.12.038.
[22] S. Bang, J. Kim, G. Yoon, T. Tanaka, J. Rho, Recent advances in tunable and reconfigurable metamaterials, Micromachines 9 (11) (2018) 560, https://doi.org/10.3390/mi9110560.
[23] L. Kurra, M.P. Abegaonkar, A. Basu, S.K. Koul, Switchable and tunable notch in ultra-wideband filter using electromagnetic bandgap structure, IEEE Microw. Wirel. Compon. Lett. 24 (12) (2014) 839–841, https://doi.org/10.1109/lmwc.2014.2363020.
[24] J. Zhao, Q. Cheng, J. Chen, M.Q. Qi, W.X. Jiang, T.J. Cui, A tunable metamaterial absorber using varactor diodes, New J. Phys. 15 (4) (2013), 043049. https://doi.org/10.1088/1367-2630/15/4/043049.
[25] S. Ghosh, K.V. Srivastava, Broadband polarization-insensitive tunable frequency selective surface for wideband shielding, IEEE Trans. Electromagn. Compat. 60 (1) (2018) 166–172, https://doi.org/10.1109/temc.2017.2706359.
[26] L. Liu, A.R. Katko, D. Li, S.A. Cummer, Broadband electromagnetic metamaterials with reconfigurable fluid channels, Phys. Rev. B 89 (24) (2014)https://doi.org/10.1103/PhysRevB.89.245132.
[27] T.S. Kasirga, Y.N. Ertas, M. Bayindir, Microfluidics for reconfigurable electromagnetic metamaterials, Appl. Phys. Lett. 95 (21) (2009), 214102. https://doi.org/10.1063/1.3268448.
[28] Y. Poo, R.-x. Wu, G.-h. He, P. Chen, J. Xu, R.-f. Chen, Experimental verification of a tunable left-handed material by bias magnetic fields, Appl. Phys. Lett. 96 (16) (2010), 161902. https://doi.org/10.1063/1.3409120.
[29] W. Liu, Y. Shen, G. Xiao, X. She, J. Wang, C. Jin, Mechanically tunable sub-10 nm metal gap by stretching PDMS substrate, Nanotechnology 28 (7) (2017), 075301. https://doi.org/10.1088/1361-6528/aa5366.
[30] P. Gutruf, C. Zou, W. Withayachumnankul, M. Bhaskaran, S. Sriram, C. Fumeaux, Mechanically tunable dielectric resonator metasurfaces at visible frequencies, ACS Nano 10 (1) (2016) 133–141, https://doi.org/10.1021/acsnano.5b05954.
[31] S. Yang, P. Liu, M. Yang, Q. Wang, J. Song, L. Dong, From flexible and stretchable meta-atom to metamaterial: a wearable microwave meta-skin with tunable frequency selective and cloaking effects, Sci. Rep. 6 (2016), 21921. https://doi.org/10.1038/srep21921.
[32] G.A. Snook, P. Kao, A.S. Best, Conducting-polymer-based supercapacitor devices and electrodes, J. Power Sources 196 (1) (2011) 1–12, https://doi.org/10.1016/j.jpowsour.2010.06.084.
[33] J. DeGraff, R. Liang, M.Q. Le, J.-F. Capsal, F. Ganet, P.-J. Cottinet, Printable low-cost and flexible carbon nanotube buckypaper motion sensors, Mater. Des. 133 (2017) 47–53, https://doi.org/10.1016/j.matdes.2017.07.048.
[34] D.S. Hecht, L. Hu, G. Irvin, Emerging transparent electrodes based on thin films of carbon nanotubes, graphene, and metallic nanostructures, Adv. Mater. 23 (13) (2011) 1482–1513, https://doi.org/10.1002/adma.201003188.
[35] K.S. Kim, Y. Zhao, H. Jang, S.Y. Lee, J.M. Kim, K.S. Kim, J.H. Ahn, P. Kim, J.Y. Choi, B.H. Hong, Large-scale pattern growth of graphene films for stretchable transparent electrodes, Nature 457 (7230) (2009) 706–710, https://doi.org/10.1038/nature07719.
[36] L. Hu, H.S. Kim, J.Y. Lee, P. Peumans, Y. Cui, Scalable coating and properties of transparent, flexible, silver nanowire electrodes, ACS Nano 4 (5) (2010) 2955–2963, https://doi.org/10.1021/nn1005232.
[37] B.W. Zhang, W.L. Li, Y. Yang, C.T. Chen, C.F. Li, K. Suganuma, Fully embedded CuNWs/PDMS conductor with high oxidation resistance and high conductivity for stretchable electronics, J. Mater. Sci. 54 (8) (2019) 6381–6392, https://doi.org/10.1007/s10853-019-03333-x.
[38] J. Jung, H. Lee, I. Ha, H. Cho, K.K. Kim, J. Kwon, P. Won, S. Hong, S.H. Ko, Highly stretchable and transparent electromagnetic interference shielding film based on silver nanowire percolation network for wearable electronics applications, ACS

Appl. Mater. Interfaces 9 (51) (2017) 44609–44616, https://doi.org/10.1021/acsami.7b14626.
[39] M.-x. Jing, M. Li, C.-y. Chen, Z. Wang, X.-q. Shen, Highly bendable, transparent, and conductive AgNWs-PET films fabricated via transfer-printing and second pressing technique, J. Mater. Sci. 50 (19) (2015) 6437–6443, https://doi.org/10.1007/s10853-015-9198-3.
[40] J.-J. Chen, S.-L. Liu, H.-B. Wu, E. Sowade, R.R. Baumann, Y. Wang, F.-Q. Gu, C.-R.-L. Liu, Z.-S. Feng, Structural regulation of silver nanowires and their application in flexible electronic thin films, Mater. Des. 154 (2018) 266–274, https://doi.org/10.1016/j.matdes.2018.05.018.
[41] P. Lee, J. Lee, H. Lee, J. Yeo, S. Hong, K.H. Nam, D. Lee, S.S. Lee, S.H. Ko, Highly stretchable and highly conductive metal electrode by very long metal nanowire percolation network, Adv. Mater. 24 (25) (2012) 3326–3332, https://doi.org/10.1002/adma.201200359.
[42] P. Liu, S. Yang, A. Jain, Q. Wang, H. Jiang, J. Song, T. Koschny, C.M. Soukoulis, L. Dong, Tunable meta-atom using liquid metal embedded in stretchable polymer, J. Appl. Phys. 118 (1) (2015), 014504. https://doi.org/10.1063/1.4926417.
[43] J.H. Choi, J. Ahn, J.B. Kim, Y.C. Kim, J.Y. Lee, I.K. Oh, An electroactive, tunable, and frequency selective surface utilizing highly stretchable dielectric elastomer actuators based on functionally antagonistic aperture control, Small 12 (14) (2016) 1840–1846, https://doi.org/10.1002/smll.201503726.
[44] W. Withayachumnankul, K. Jaruwongrungsee, A. Tuantranont, C. Fumeaux, D. Abbott, Metamaterial-based microfluidic sensor for dielectric characterization, Sensors Actuat. A Phys. 189 (2013) 233–237, https://doi.org/10.1016/j.sna.2012.10.027.